Characterization of double network epoxies with tunable compositions

Andrew T. Detwiler · Alan J. Lesser

Abstract This article reports the processing and characterization of epoxy resins with near constant molar cross-link density prepared from sequentially reacted amine cross-linking agents. Stoichiometric blends of curing agents with compositions ranging from all polyetheramine to all diaminodiphenylsulfone (DDS) are reacted with an epoxy monomer in a staged curing procedure. The low reactivity of the aromatic amine permits the selective reaction of the aliphatic amine in the first stage. The residual aromatic amine and epoxide functionality are reacted in a second stage at higher temperature. Above approximately 50% DDS content the first stage produces sol glasses which have not reached the gel point. The glass transition temperatures of the partially cured networks decrease monotonically with increasing DDS content. The partially cured networks can be characterized thermally and mechanically above their respective glass transitions without significantly advancing the reaction of the residual DDS and epoxide functionality. The networks formed after the second stage of the cure exhibit thermal and mechanical properties intermediate between those of the two individual amine cured networks, according to composition. The blends do not show any evidence of phase separation across the entire composition range in either the partially cured or fully cured state.

Introduction

Amine cured epoxies are widely used as coatings, structural adhesives, and encapsulants for a variety of applications [1]. By changing the nature of the epoxide and amine monomers it is possible to dramatically alter the physical and mechanical properties of the resulting networks. Although a variety of epoxide monomers are available, the diglycidylether of bisphenol A (DGEBA) and its oligomers are the most widely employed resins. On the other hand, there are comparatively far more curing agents available to react with the epoxides. The choice of curing agent is highly application driven since glass transition temperature (T_g), solvent resistance, color, toughness, strength, and a number of other properties can be tailored by the choice of curing agent.

Aliphatic polyetheramine (PEA) curing agents are often employed when tough resins are needed and solvent resistance or high temperature properties are not critical. Diaminodiphenylsulfone (DDS) cured epoxies have excellent thermal stability and solvent resistance, but they tend to be brittle. They are often blended with high T_g thermoplastics to form phase separated composites with increased fracture toughness [2]. There is relatively little published work on the physical and mechanical properties of blends of amine curing agents. Blends of PEAs have been studied in terms of the heterogeneity of the networks they form under various curing conditions [3–5]. Aromatic diamines have been blended together to form low viscosity eutectics that facilitate mixing with epoxy resins at lower temperatures [6]. Others have used blends of aromatic amines in order to control reaction kinetics and the incipient phase separation of thermoplastic additives [7]. B-staged epoxy prepreg materials often contain blends of amines and/or other latent curing agents where differences in reactivity are critical to shelf life and material handling characteristics [8, 9]. However, detailed analyses of relationships between physical properties, including nonlinear mechanical properties, composition, and processing schemes in these systems are rare [5, 10].

Part of the motivation for this work comes from recent studies in the literature where combinations of different

A. T. Detwiler · A. J. Lesser (✉)
University of Massachusetts Amherst, 120 Governors
Dr., Amherst, MA 01003, USA
e-mail: ajl@polysci.umass.edu

monomers in hydrogels, advanced processing techniques in prestressed elastomers, and additives in IPNs have been exploited to create polymeric double network systems with improved properties. The double network hydrogels use combinations of rigid and flexible monomers to create hydrogels with increased fracture toughness. The order of network synthesis steps as well as the interconnectivity of the networks was observed to dramatically affect the properties of the final materials [11]. Similarly, prestressed double network elastomers have been reported where a thermoplastic elastomer is stretched and cured by radical cross-linking while it is in the stretched state [12]. This processing procedure generates networks with interesting stress–strain and thermal properties. However, little work has investigated double network glasses outside of phase separated systems. Single phase interpenetrating networks (IPNs) of polystytrene have been reported [13]. One significant limitation of these systems is their reliance on specific chemistries with little flexibility in the synthesis and processing procedures. As noted above, epoxies offer significant flexibility in both of these aspects, thus allowing structure–property relationships to be explored across a wide range of network architectures and chemical functionalities.

In this work we investigate the basic physical and mechanical properties of double network epoxies formulated using stoichiometric blends of aromatic and aliphatic amine curing agents. The curing agents are selected to have very similar molecular weight and to maintain miscibility of the mixtures at all conversions over the entire range of aromatic to aliphatic amine ratios. Effort is made in this paper to relate basic physical and mechanical properties to network architecture.

Method

Stoichiometric mixtures of DGEBA $M_E = 175$ g/mol, DER 332, supplied by Dow; 4,4′-diaminodiphenylsulfone (DDS) 97%, from Acros $M_A = 62$ g/mol; and a,ω-diaminopolypropyleneoxide (PEA), Jeffamine D230, courtesy of Huntsman $M_A = 60$ g/mol are prepared. The chemical structures of the monomers are given in Fig. 1.
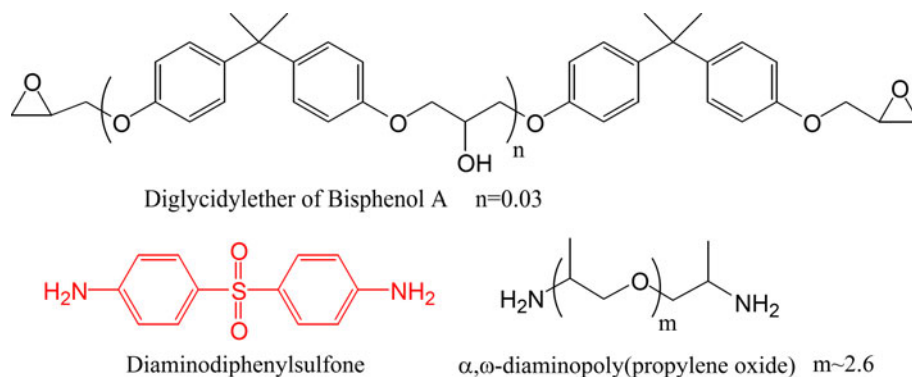
The DDS fraction of the curing agents (ϕ) is varied from 0 to 1 for different blends while maintaining stoichiometry between the amine and epoxide functionalities. The DDS component is stirred into DGEBA under vacuum at 125 °C until it dissolves. The solution is cooled to 80 °C before the PEA component is stirred in, and the mixtures are quickly poured into cylindrical glass molds (11.5 mm internal diameter) treated with a release agent (Sufasil, Pierce Chemicals). The molds are placed in a nitrogen-purged oven at 100 °C for 6 h. Half of the molds containing each blend are cooled to room temperature in a water bath, and half are postcured at 200 °C for 6 h before being cooled in a similar manner. Samples with $\phi = 0.8$, 0.9, and 1.0 are postcured for 4 h at 200 °C and for 2 h at 220 °C. All samples are stored in their molds in a freezer at −10 °C until use.

The T_g of each resin is determined as the inflection point of the heat flow versus temperature (dH/dT) curve from heating 5 mg samples at 10 °C/min in a DSC 2910 (TA Instruments). All samples from DSC are taken from bulk cast samples. Conversion is measured from the integration of the exotherm in the dH/dT curves. Density is measured at 21 °C by the water displacement method (ASTM D792).

Samples for dynamic mechanical thermal analysis (DMTA) are machined to Length × Width × Thickness of $30 \times 5 \times 0.5$ mm^3 for testing using single cantilever beam and tension geometries. Testing is conducted using a DMTA 2980 from TA Instruments at 1 Hz, 15 μm displacement and a ramp rate of 3 °C/min from −120 to 280 °C. The storage modulus (E'), loss modulus (E''), and loss tangent (tan δ) are recorded as a function of temperature. The full width at half-maximum (FWHM) is calculated from tan δ in the α-transition region, where the limits are taken as the minimum between T_β and T_g and the maximum associated with the α-transition.

X-ray scattering is conducted on an evacuated Rigaku Molecular Metrology SAXS instrument using the CuK$_\alpha$ spectral line with wavelength $\lambda = 0.1542$ nm, excited by

Fig. 1 Epoxy resin and amine cross-linkers

Diglycidylether of Bisphenol A   n=0.03

Diaminodiphenylsulfone

α,ω-diaminopoly(propylene oxide)   m~2.6

45 kV and 0.67 mA. The slit collimated beam has a square cross-section of 0.3×0.3 mm. The detector for small angle X-ray scattering (SAXS) is a gas-filled 2D Multiwire detector, and the sample-to-detector length is $L = 1477$ mm as calibrated by the $q = 1.076$ nm^{-1} peak from a silver behenate standard. Here, $q = 4\pi/\lambda \sin\theta$ and 2θ is the scattering angle. Wide angle X-ray scattering (WAXS) is conducted on the same instrument, but a Fujifilm CR HR-V image plate at $L = 139$ mm is used to record the scattering. L is calibrated using the $q = 15.197$ nm^{-1} 110 peak from a tricosane standard. The scattering intensities are transferred to a computer using a Fujifilm Bas-2500 image reader at 200 μm resolution, 16 bit gradation, and a dynamic range of 30,000. Scattering patterns from SAXS and WAXS are circularly integrated to give scattering profiles with intensity in arbitrary units versus q in nm^{-1}.

For compression testing, samples are removed from the molds and machined into compression bullets with a height to diameter ratio of 1:1. A drop of soapy water is placed on each face of the bullets and on the compression platens. PTFE film is placed on the top and bottom faces of the bullets. An Instron 5800 universal tester is used to for compression testing at 20 °C using a constant true strain rate of 1.67×10^{-3} s^{-1}. Elevated temperature compression experiments are conducted on the same instrument in a nitrogen-purged oven that surrounds the compression platens. Samples are equilibrated at the testing temperature for 30 min prior to testing. High molecular weight silicone oil is used as the liquid lubricant at elevated temperatures.

Results and discussion

Partially cured networks

In this work we use DDS as a latent curing agent such that the aliphatic amine and a corresponding fraction of the epoxide form a partially cured network after the initial cure stage at 100 °C. In all cases the unreacted DDS and epoxide components act to reduce the T_g of an otherwise fully cured aliphatic amine cured network. The depression of T_g with increasing DDS fraction in the partially cured networks is clear from the plots of the storage modulus (E') versus temperature in Fig. 2.

Closer inspection of E' in the glassy state also shows that E' increases with DDS fraction. The presence of both decreased T_g and increased E' with increasing DDS fraction indicates that the unreacted epoxy and DDS components act as internal antiplasticizers for the aliphatic network [14, 15]. In Fig. 3 the low segmental mobility below T_g is evidenced by the strong decrease in the strength of the β-transition with increasing DDS fraction. Since segmental mobility is depressed below T_g
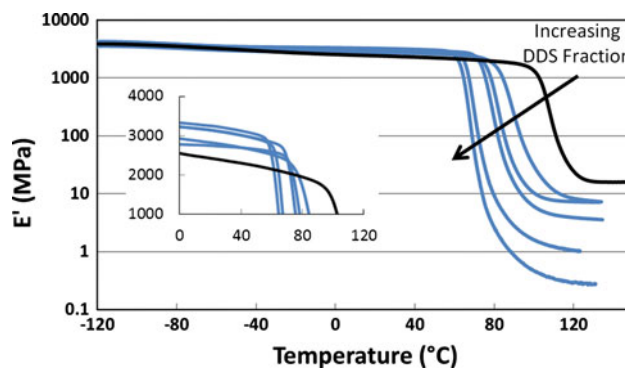

Fig. 2 Plot of storage modulus versus temperature from DMTA temperature scans of partially cured networks. *Arrow* highlights the decrease in T_g and E'_R with increasing DDS content. *Inset* highlights increase in glassy storage modulus with increasing (unreacted) DDS fraction
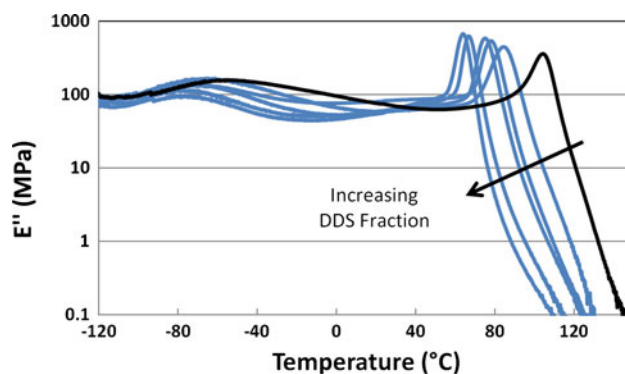

Fig. 3 Plot of loss modulus versus temperature from DMTA temperature scans on partially cured networks. The *arrow* indicates the trend of decreasing T_a with increasing DDS content. There is also a clear decrease in the amplitude of the β-transition in the vicinity of -60 °C. Both trends are consistent with internal antiplasticization in a partially cured epoxy

(antiplasticization), the glassy moduli of partially cured materials is higher than that of fully cured materials. The networks formed in the first stage of the curing scheme are effectively epoxide rich formulations with an additional unreactive diluent in the form of the unreacted DDS, which is in stoichiometric balance with the unreacted epoxide functionality. The presence of a single glass transition in DMTA temperature scans (Fig. 3) indicates the partially cured networks are miscible and contain a single phase. DMTA measurements were unable to be obtained in either tension or single cantilever beam geometries on samples where the DDS content was greater than 50% due to sample failure during clamping.

Partially cured epoxy resins fabricated from low molecular weight epoxide and amine monomers are notoriously difficult to machine or test mechanically in the glassy state until the conversion is well beyond the critical conversion [14–16]. For a difunctional epoxy and
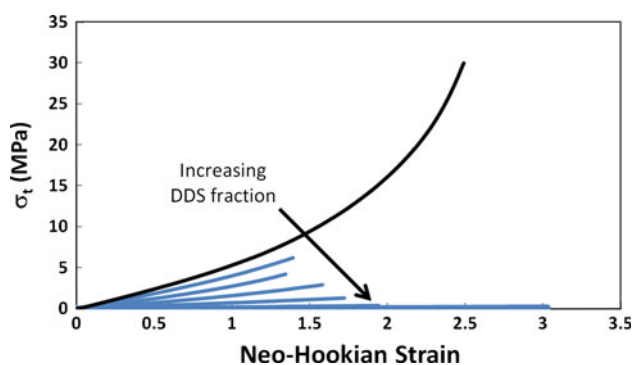
J Mater Sci (2012) 47:3493–3503

Fig. 4 Graph of true stress versus neo-Hookian strain from uniaxial compression testing of partially cured networks. Testing was done at 120 °C to measure the rubbery responses of the networks

tetrafunctional amine the critical conversion is ∼0.58 [17]. For compositions with greater than 50% DDS the conversion after the first cure stage falls below the gelation threshold, so the materials are extremely brittle sol glasses.

Figure 4 is a plot of true stress versus neo-Hookian strain from compression tests run on samples at 120 °C after the first stage of the cure. Based on DSC and DMTA results, 120 °C is well above T_g for all networks after the first stage of curing so they should behave as rubbers, as opposed to glasses.

The sample with only the aliphatic curing agent is fully cured, whereas the majority of the DDS, in networks that contain it, remains unreacted. Samples that contain greater than 50% DDS behave as viscous liquids because they do not yet have topologically percolating cross-linked networks. The low strain moduli scale inversely with DDS content, as expected for systems with increasingly diluted network chains. However, the networks with unreacted DDS ($0 < \phi < 0.6$) tend to fail at relatively low strains. This failure behavior indicates the low connectivity of the partially cured networks imparts low cohesive strength, even in the rubbery state.

Fully cured networks

The partially cured materials are postcured at 200 °C (additional step at 220 °C for samples with greater than 80% DDS). They show no change in T_g between the first and second temperature sweeps in DSC, which indicates they are fully cured. The T_g values, measured from DSC, of the fully cured networks are compared those of the partially cured networks in Fig. 5.

Clearly, T_g increases with DDS fraction in the fully cured networks, and this trend is the same whether T_g is measured thermally or mechanically. Figures 6 and 7 show how the storage and loss moduli curves change systematically with DDS fraction. Unlike the partially cured
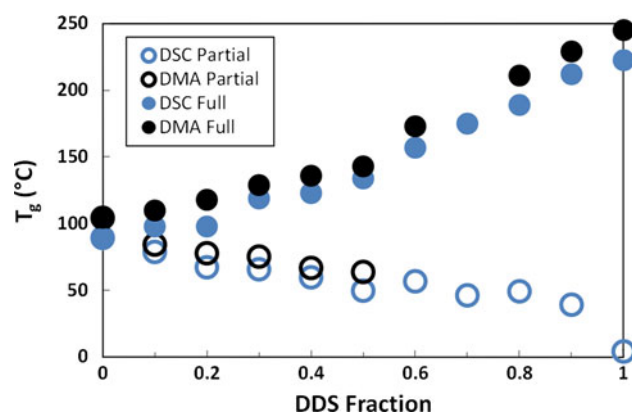

Fig. 5 Graph of T_g of double networks as a function of DDS fraction. Data from DSC (light) and DMTA (dark) are from measurements made after the first (open symbols) and second (closed symbols) cure stages
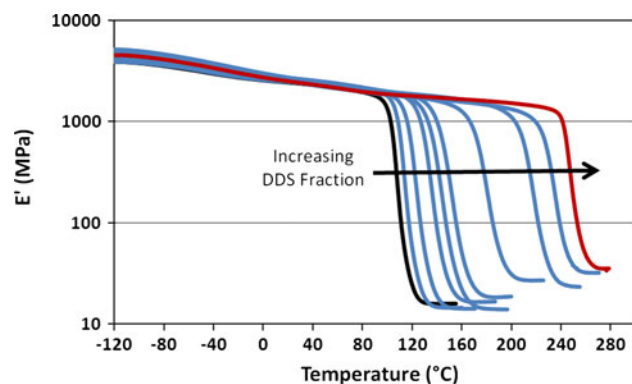

Fig. 6 Plot of storage modulus versus temperature scans from DMTA analysis. The arrow indicates the direction of increasing DDS content. The trend is for increasing α-transition temperature and plateau modulus with increasing DDS content

networks, the fully cured networks have nearly identical α-transitions across the composition range as shown in Fig. 7. T_g shifts to higher temperatures with increasing DDS, and the breadth of the transition increases. However, there is no splitting of the loss modulus into two α-transition peaks. A single α-transition indicates that the networks remain miscible across the entire composition range.

The α-transition appears to be narrowest for the pure aliphatic and pure aromatic compositions based on the normalized and shifted loss modulus curves presented in Fig. 8. As blends approach 50% of either component the α-transition becomes much broader, particularly on the low temperature side of the transition.

This relationship has been observed in epoxies cured with blends of m-phenylenediamine and PEA [10]. The broader α-transition associated with the blends indicates that the pure networks are more homogeneous than the blended networks [18]. Heterogeneity, as measured by the breadth of the
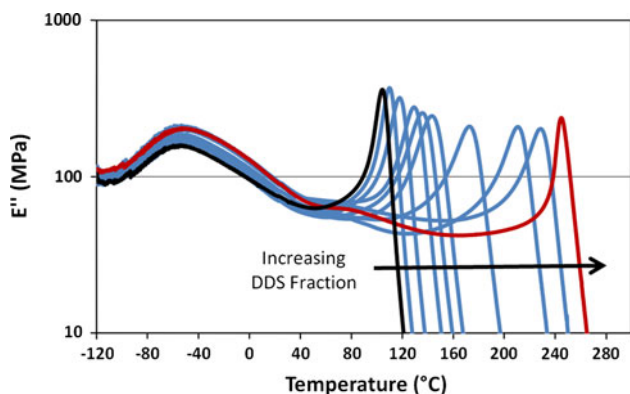
3496

Springer

Fig. 7 Plot of loss modulus versus temperature scans from DMTA analysis. The *arrow* indicates the direction of increasing DDS content. The trend indicates that the α-transition temperature increases and there is no change in the β-transition temperature with increasing DDS content
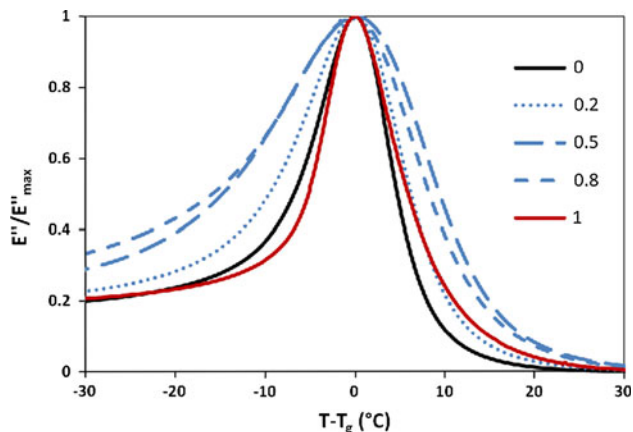

Fig. 9 Graph showing full width at half-maximum versus DDS fraction from the α-transition region of DMTA temperature scans. Partially cured (*hollow circles*) and fully cured networks (*filled circles*). FWHM increases in proportion to the heterogeneity of segmental mobility on the timescale of the 1 Hz oscillations

Fig. 8 Normalized loss modulus versus shifted T_g plotted from DMTA temperature scans of selected network compositions. The temperature is shifted by the temperature at which the loss modulus exhibits a maximum during the α-transition. The loss modulus is normalized by the maximum value of the loss modulus during the α-transition

α-transition, arises due to the differences in local segmental mobility associated with the two different curing agents. The change in breadth of the α-transition is quantified by measuring the FWHM of the loss modulus peak in the α-transition region. Data for FWHM are presented in Fig. 9.

Heterogeneity in double network epoxies can result from different combinations of topological connectivity. An epoxide monomer may react with zero, one, or two DDS molecules. Therefore, counting only nearest neighbor connectivity, there are three types of epoxide segments in the networks. However, the α-transition, occurring on the time scale of seconds [19], has been shown to arise from the cooperative motions of at least 10–20 atoms in the polymer chain [20, 21]. This cooperative region can contain a significantly larger number of combinations of
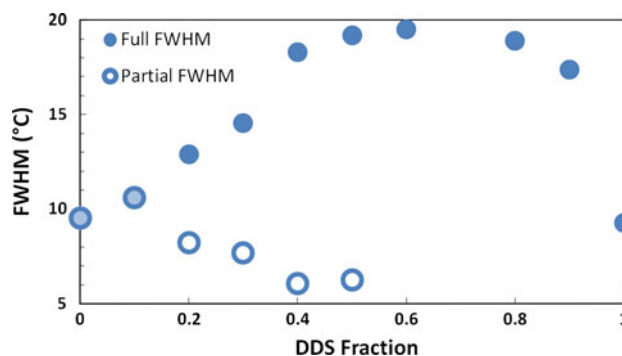
aliphatic and aromatic components, so the distribution of aliphatic and aromatic cross-linkers can cause molecular scale dynamic heterogeneity. The two-stage cure schedule promotes this molecular scale heterogeneity. The aliphatic amine components all react in the first stage, and there is the potential to form large clusters of aliphatic amine-rich regions. The DDS and DGEBA that remain unreacted must permeate these clusters because there is no evidence of more than one T_g. However, this topological heterogeneity can have important contributions to toughening a single phase epoxy, as demonstrated by Wu et al. [5]. The fracture behavior of these networks will be investigated in a second paper in this series.

X-ray scattering

Although WAXS and SAXS are sensitive to local density fluctuations in a material, they are not able to provide information about compositional heterogeneity on the segmental level in most amorphous materials [4, 5]. Both WAXS and SAXS data indicate that the samples are amorphous due to the absence of sharp scattering peaks. In the WAXS scan presented in Fig. 10 the broad peaks arising from the amorphous halo are the most prominent features [22].

The low q peak is shifted to lower q for the blended system, which indicates that the length scale of the electron density contrast increases slightly in networks of blended amines relative to networks composed of a single curing agent. These peaks arise at $q = 6.8$ nm^{-1} and $q = 8.3$ nm^{-1} or length scales of slightly less than 1 nm. This corresponds to the size scale of the monomer units, which should exhibit a characteristic length scale and electron density contrast due to compositional differences [23].
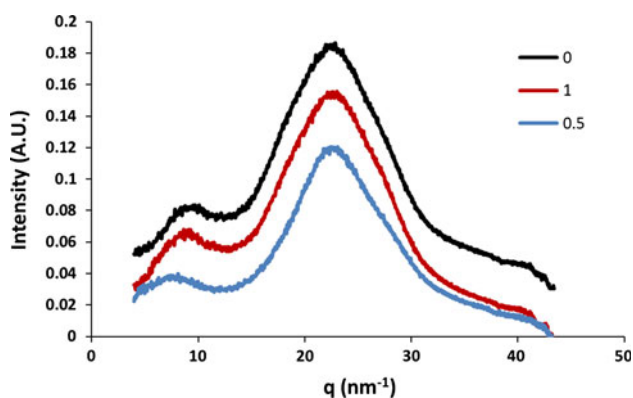
Fig. 10 Graph showing wide angle X-ray scattering profile versus scattering vector from fully cured networks. DDS fractions of 0 (*upper*), 1 (*middle*), and 0.5 (*lower*). The broad amorphous halo depicted with no sharp scattering peaks indicates that the networks are amorphous
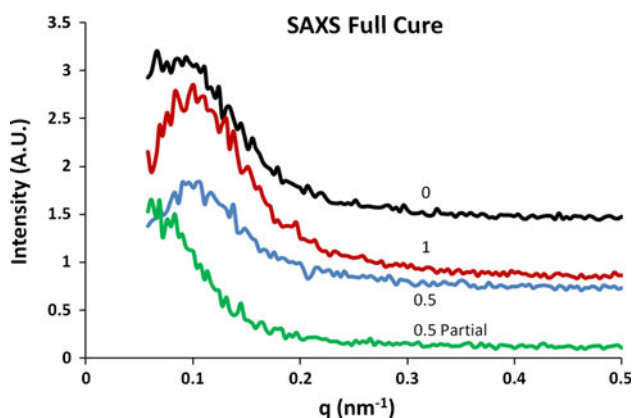

Fig. 11 Plot of small angle X-ray scattering profile versus scattering vector from fully cured networks. DDS fractions of 0, 1, 0.5, and a partially cured network with 0.5 DDS, as labelled in the figure. The increase in scattered intensity in all profiles is attributed to the approach to the beam stop. No peaks arising from large scale structures are resolved in this q range, as expected from an amorphous single phase material

The SAXS data presented in Fig. 11 also indicate that the networks are amorphous, with no long range order. The only feature resolvable from the scattering profile is the increase in scattering at low q, which is attributed to the approach to the beam stop. Therefore, the X-ray scattering data are consistent with the conclusion that these double network epoxies are single phase miscible systems across the composition range.

Compression testing

Affine deformation in compression probes both the pre- and post-yield responses of materials. In contrast to

uniaxial extension, uniaxial compression does not create a neck or promote fracture that otherwise complicates the analysis of the true stress–true strain responses of polymers [24]. Below T_g, the low strain response of polymers is sensitive to their thermomechanical history and local segmental dynamics [25, 26]. The high strain response, beyond the yield strain, is sensitive to cross-link density in thermosets [27] and entanglement density in thermoplastics [28]. There is some debate in the literature in terms of how to characterize the high strain response of thermoplastics and thermosets. Although the strain hardening response has been shown by numerous authors to correlate with entanglement density or cross-link density [29, 30], the mechanical response does not scale with temperature or strain rate as one might predict from rubber elasticity arguments [28, 31]. The discrepancy arises from the intermolecular interactions present during inelastic deformation, and the viscous dissipation of strain energy is, predictably, rate and temperature dependent [28, 31]. Haward and Thackaray proposed that glassy polymers undergoing post-yield deformation should behave like cross-linked elastomers where entangled chains in the glass are analogous to cross-linked chains in a rubber [32]. Strain hardening is, thus, thought to result from the loss of entropy as entangled chains align [30]. This non-linear behavior can be captured by using a neo-Hookian measure of strain [30, 33]. Here, the strain hardening modulus (G_R) is the slope of the true stress (σ_t) versus neo-Hookian strain curve as given by Eq. 1.

$$G_R = \partial \sigma_t / \partial \left(\lambda^2 - 1/\lambda \right) \quad (1)$$

where λ is the extension ratio. M_c is calculated from the strain hardening response using Eq. 2, or from stoichiometric considerations using Eq. 3,

$$M_c = \phi \rho R T / G_R \quad (2)$$

$$M_c = 2(M_E + M_A) \quad (3)$$

where ρ is the mass density, R is the ideal gas constant, T is the absolute temperature, and ϕ is a constant related to cross-link mobility and is assumed to be equal to 1 for immobile cross-links [34]. M_E is the epoxide equivalent weight and M_A is the amine equivalent weight.

Equations 1 and 2 provide a way to interpret the strain hardening responses of networks in terms of network architecture [32, 35]. The strain hardening modulus is the value of the slope of the true stress–neo-Hookian strain curve (Eq. 1) measured at 90% of the ultimate true strain. Using the slope at 90% of the ultimate true strain (ε_b) allows one to sample G_R at a standardized location deep in the non-linear deformation region, where the connectivity of cross-links should have the greatest relative influence over the change in true stress with increasing strain.
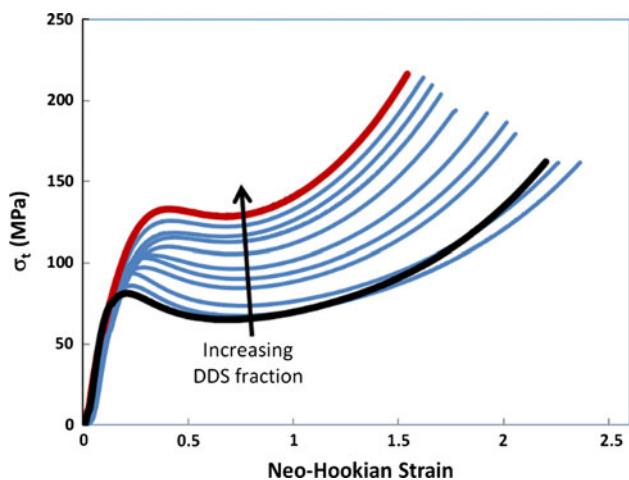
Fig. 12 Plot of true stress versus neo-Hookian strain from uniaxial compression tests on fully cured networks conducted at 20 °C. Increasing DDS content shifts the curves to higher stresses and decreases the strain at which the networks fail, but the qualitative shape of the curves is unchanged
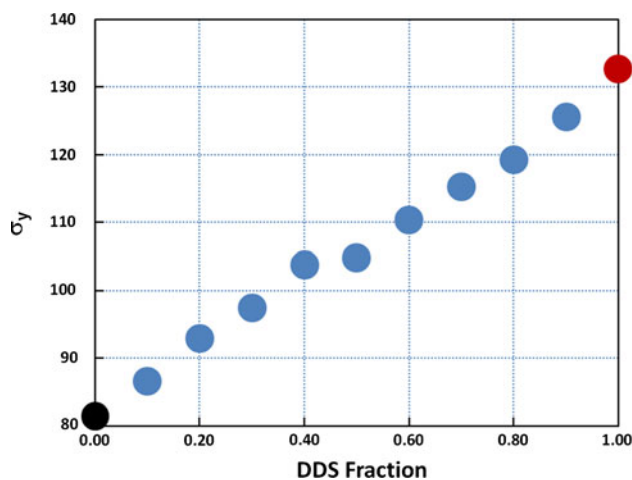

Fig. 14 Plot of yield stress versus DDS fraction. Yield stress increases in proportion to DDS fraction
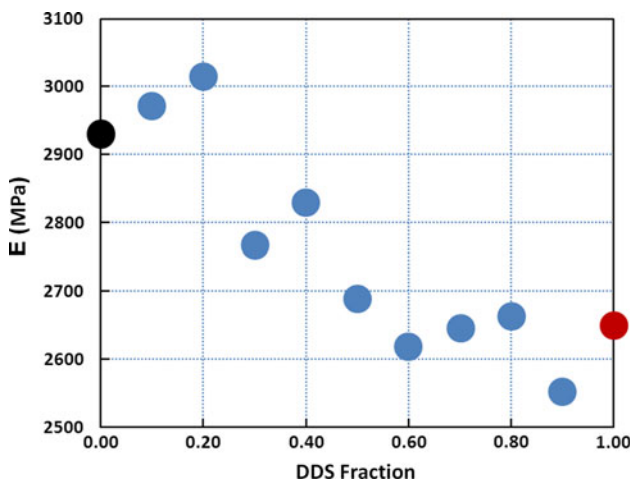

Fig. 13 Graph of compressive modulus versus DDS fraction measured at 20 °C. Modulus decreases with increasing DDS content

Equation 2 uses the strain hardening response to calculate the molecular weight between cross-links.

Although the strain hardening responses of a number of glassy polymers correlate with entanglement or cross-link density, as calculated from the plateau modulus [35], the theory fails to account for the temperature and strain rate dependence of strain hardening, as well as the ~ 2 order of magnitude quantitative discrepancy in the calculated entanglement density [16, 28, 36, 37]. On these grounds, strain hardening is thought to originate from a combination of local segmental interactions, and the larger scale entanglement network, which both depend on temperature and the number of segments between entanglements [36]. Changes in chain conformation during large deformations

cause the relative contributions of intersegmental interactions and network connectivity to change. It has proven to be challenging to identify individual contributions experimentally [36, 38].

Most work on the large strain mechanics of glassy polymers has focused on thermoplastics, such as PC, PS, PPO, PMMA, and PETG [39]. A few authors have looked at cross-linked systems such as cross-linked PS [28], cross-linked PMMA [38], and epoxies [16, 27, 40]. Particularly in epoxy systems, the molecular weight between cross-links (hundreds of g/mol) is on the order of a tenth of the entanglement molecular weight of thermoplastics (thousands of g/mol). Therefore, the cross-links in epoxy resins are expected to affect local segmental mobility at a much smaller scale than the entanglements of thermoplastics. This reduction in segmental mobility is the main reason T_g increases with cross-link density [41].

Uniaxial compression tests on fully cured samples in Fig. 12 demonstrate that the networks exhibit qualitatively similar true stress–neo-Hookian strain responses across the entire composition range, but the curves are shifted to higher stresses with increasing DDS content in the non-linear deformation region. The elastic modulus, measured at small strains, decreases with DDS fraction as demonstrated in Fig. 13. This inverse relationship between T_g and elastic modulus has been observed in other fully cured epoxy systems [42] where the glassy modulus is inversely proportional to the intensity of the low temperature β-relaxation. The trends of loss modulus with DDS fraction in Fig. 7 are consistent with this explanation.

Figure 14 indicates that yield stress increases with DDS content. Yield is a stress induced thermally activated transition from low segmental mobility to high segmental mobility [43]. It is sensitive to localized segmental interactions such as Van der Waals forces and hydrogen
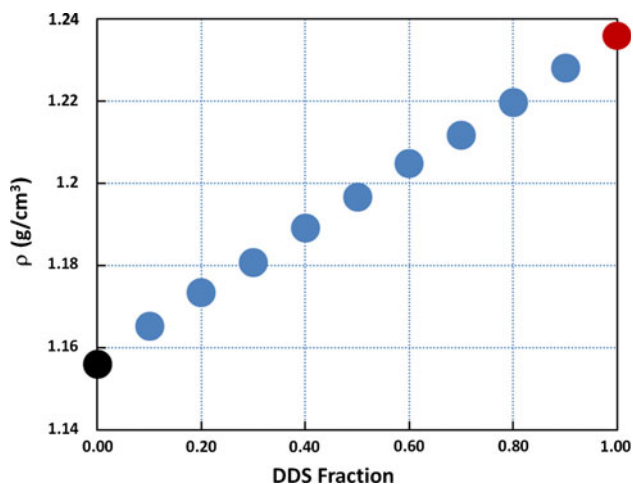
Fig. 15 Plot of density versus DDS fraction measured by the water displacement method at 21 °C. Density increases linearly with DDS fraction
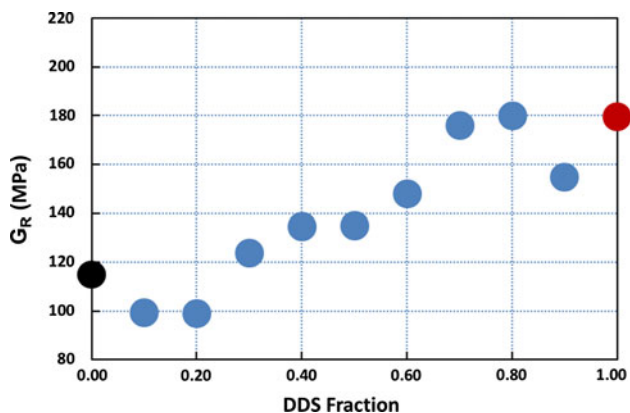

Fig. 16 Plot of strain hardening modulus versus DDS fraction. The strain hardening modulus at 90% of the ultimate strain increases with DDS content. This trend indicates the DDS fraction increases the stiffness of networks relative to the aliphatic fraction
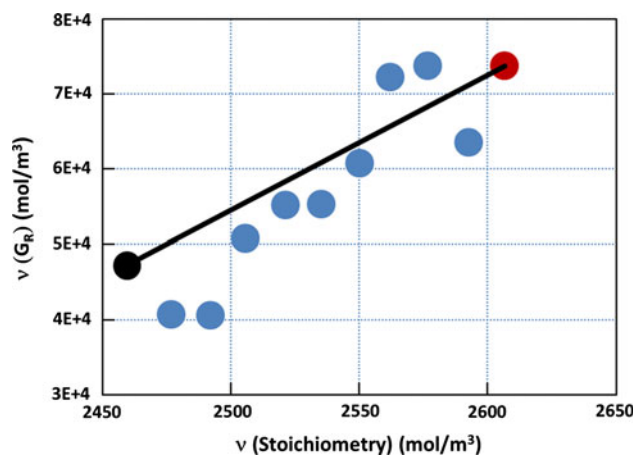

Fig. 17 Plot of cross-link density calculated from the strain hardening modulus versus cross-link density calculated from the stoichiometric balance of monomers. Both measures of cross-link density are functions of the mass density of the networks, which increases with DDS fraction. The *black line* has a slope of ∼180, which indicates that $v(G_R)$ increases much faster than would be expected from stoichiometric considerations

bonding that restrict segmental mobility. These non-covalent interactions are functions of density, thermomechanical history, chemical composition, and test temperature [25, 44–46]. Since the chemical compositions of the networks vary it is difficult to quantitatively describe the thermomechanical histories of the samples except to say that they have all experienced a similar aging time (several days) and temperature (−10 °C). Under these conditions, physical aging is expected to be a relatively slow process, occurring over thousands of hours [47, 48].

Since both density in Fig. 15 and T_g in Fig. 5 increase with increasing DDS fraction, one would correctly predict that yield stress increases with DDS content as well. These double network epoxy systems allow for precise control over physical and mechanical properties, such as T_g, yield

stress, and density by simply changing the DDS fraction in the networks.

It has been argued in the thermoplastic [32, 33] and thermoset literature [16, 27] that the strain hardening modulus, measured in the glassy state, scales with entanglement density and cross-link density, respectively. The DDS and aliphatic curing agents used in this study were selected, in part, because they have nearly identical molecular weight. Therefore, changes in the composition should not affect the molar cross-link density.

However, the strain hardening responses of the double network epoxies in Fig. 16 do show dependence on DDS content. Since the mass density increases with DDS content, the cross-link density, in terms of cross-links per unit volume, does increase with DDS content.

The cross-link density, as calculated from G_R, is plotted in Fig. 17 against the cross-link density calculated from stoichiometric considerations. The slope of the line between the all aliphatic and all aromatic networks has a slope of approximately 180. Clearly, the cross-link density calculated from the strain hardening modulus increases with DDS content faster than it does based on stoichiometric considerations. This behavior reaffirms the notion that the strain hardening response depends on both cross-link density and the chemical nature of the cross-links and the chain segments between them in the glassy state.

The true stress versus neo-Hookian strain curves of fully cured networks tested 20 °C above T_g are plotted in Fig. 18. In the low strain region the true stress is a linear function of strain. However, the data in Fig. 19 show that the shear modulus (G), from the linear portion of the curves, increases with DDS content. A linear relationship between the true
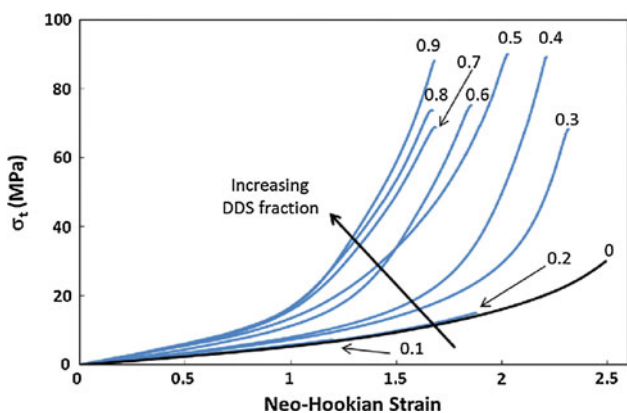
Fig. 18 Plot of true stress versus neo-Hookian strain from compression tests conducted at $T_g + 20$ °C for double networks. The *arrow* indicates the trend of increasing stiffness at large strains with increasing DDS fraction
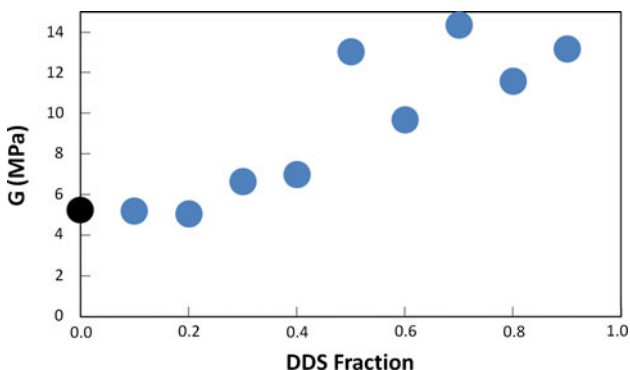

Fig. 19 Graph showing compressive modulus versus DDS fraction measured in the low strain region of compression tests conducted at $T_g + 20$ °C. The increase in the low strain rubbery modulus with DDS fraction indicates that the DDS component of the networks increases the apparent cross-link density relative to the polyether-amine component
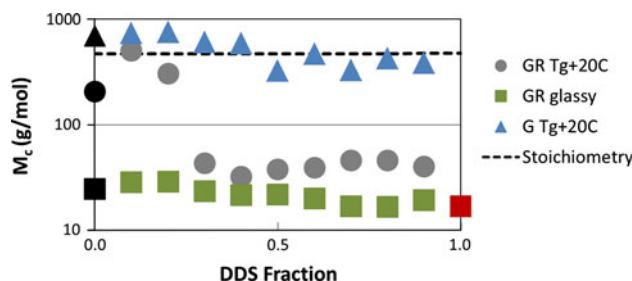

Fig. 20 Plot of molecular weight between cross-links versus DDS fraction. M_c is calculated using four different data sets: strain hardening modulus of compression curves acquired at $T_g + 20$ °C (*circles*), strain hardening modulus of compression curves tested at 20 °C (*squares*), low strain modulus of compression curves acquired at $T_g + 20$ °C (*triangles*), stoichiometric calculations based on tetrafunctional cross-links (*dashed line*)

stress and neo-Hookian strain is predicted for a Gaussian network [30]. The strong strain hardening above $-(\lambda^2 - 1/\lambda) = 1$ indicates a departure from linear behavior. This trend confirms that the composition affects the mechanical behavior, even at elevated temperature, where large thermally induced segmental fluctuations diminish the effects of intersegmental interactions. If the rubbery modulus, obtained from elevated temperature compression tests (E_R) is substituted for G_R in Eq. 2, the resulting M_c values can be calculated.

Figure 20 compares the M_c values obtained from the strain hardening modulus, obtained in both the glassy and rubbery state; the low strain shear modulus from the rubbery state, and the value calculated from stoichiometric considerations according to Eq. 3 (labeled stoichiometry in Fig. 20).

The M_c values calculated from the low strain modulus measurements obtained above T_g are in relatively good quantitative agreement with the stoichiometrically calculated values. Although the mechanical measures of M_c all have qualitatively similar trends with respect to changing DDS content, measuring the mechanical response of networks with varying compositions in the glassy state clearly introduces large quantitative discrepancies.

The effects of cross-linker structure on rubber elasticity have been studied by numerous authors over many years [34, 49, 50]. Differences in mechanical response as a function of composition in the current networks likely arise from differences in cross-link mobility, which is related to the chemical structures of the cross-linker units. The DDS amine groups are attached to rigid and bulky phenylene groups which reduce cross-link mobility relative to the secondary carbon, and relatively flexible poly(propylene oxide) chains of the aliphatic amines [34]. Reduced cross-link mobility increases the stiffness of a material for a given cross-link density [26, 27, 40], which is in agreement with the observed compression response of the double network epoxies above T_g.

Although DDS and the aliphatic diamine have similar molecular weights, they have approximately 4 and 11 rotatable bonds along their backbones, respectively, as counted by Bicerano [51]. Several authors have argued that the number of rotatable bonds between cross-links, as opposed to M_c or ν, is ultimately responsible for correlations between M_c, T_g, and mechanical properties [34, 52]. The decrease in the number of rotatable bonds with increasing DDS content in the double networks explains the increase in rubbery modulus with DDS content. Also, the greater extensibility of the aliphatic amine-rich networks, as measured by the strain at break from compression tests (Fig. 21), correlates well with the presence of more rotatable bonds in those networks. The upturn in the true stress versus neo-Hookian strain curves occurs at higher strains as the DDS fraction decreases. This dramatic increase in the modulus at large strains is observed in other
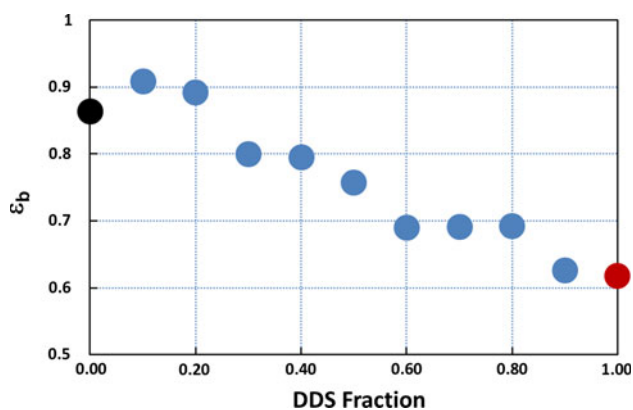
Fig. 21 Graph of true strain at break versus DDS fraction from compression testing. The decrease in strain at break with increasing DDS fraction indicates that the DDS fraction reduces the extensibility of the networks. This is evidence of the rigid nature of the diphenylsulfone segments relative to the polyether segments in the aliphatic amine

elastomeric systems at high extensions where it is attributed to the finite extensibility of chain segments.

Since the DDS segments have fewer rotatable bonds than the ether–amine segments, the shirt from linear stress–strain behavior to strain hardening is expected to take place at lower strains for networks with higher DDS fractions.

Conclusions

Double network epoxies cured in a two-stage process with varying ratios of aromatic and aliphatic amines form model network systems with tunable physical and mechanical properties. The networks formed by the reaction of the aliphatic amine component at 100 °C show strong evidence of internal antiplaticization below T_g. Above T_g, the partially cured networks behave as elastomers with rubbery moduli that depend on network connectivity. The fully cured networks are characterized by compositionally dependent modulus, yield, post-yield, and thermal properties. The difference in molecular architecture between the two curing agents leads to a broadening of the α-transition in the blended networks. This heterogeneity plateaus when the DDS forms the majority of the amine component. The yield and rejuvenated stresses increase linearly with DDS content, which indicates the sensitivity of these two parameters to intersegmental interactions in the glassy state. The strain hardening moduli in both the glassy and rubbery states increase with DDS content. However, the mechanical properties of the networks are strongly affected by intersegmental interactions in the glassy state. The connectivity of the networks, as measured mechanically, is most accurately calculated from the linear portion of true

stress versus neo-Hookian strain curves measured above T_g. A second paper in this series will evaluate the fracture behavior of double network glasses as a function of composition.

References

1. Ellis B (1993) Chemistry and technology of epoxy resins. Chapman and Hall, New York
2. Bucknall CB, Partridge IK (1983) Polymer 24(5):639
3. Wu WL, Bauer BJ (1989) Polymer 30:1384
4. Beck Tan NC, Bauer BJ, Plestil J, Barnes JD, Liu D, Matejka L et al (1999) Polymer 40:4603
5. Wu WL, Hu JT, Hunston DL (1990) Polym Eng Sci 30(14):835
6. Philipson J (1959) Method and composition for curing epoxy resins. Patent 2891927
7. Lahlali N, Naffakh M, Dumon M (2005) Polym Eng Sci 45:1581
8. Wiggins PL (1988) Epoxy curing agent composition. USA patent 4,775,736
9. Tesch H, Heym M, Doerflinger W, Stutz H, Neumann P, Nissen D, et al (1988) Curable compositions based on epoxy resins. USA patent RE32,628
10. de Nograro FF, Llano-Ponte R, Mondragon I (1996) Polymer 37(9):1589
11. Nakajima T, Furukawa H, Tanaka Y, Kurokawa T, Osada Y, Gong JP (2009) Macromolecules 42:2184
12. Singh NK, Lesser AJ (2010) Macromolecules 44:1480
13. Thiele JL, Cohen RE (1979) Polym Eng Sci 19(4):284
14. Bellenger V, Dhaoui W, Verdu J (1990) Polym Eng Sci 30(6):321
15. Jordan C, Galy J, Pascualt JP (1992) J Appl Polym Sci 46:859
16. Detwiler AT, Lesser AJ (2010) J Appl Polym Sci 117:1021
17. Flory PJ (1941) J Am Chem Soc 63:3083
18. Cook WD, Scott TF, Quay-Thevenon S, Forsythe JS (2004) J Appl Polym Sci 93:1349
19. Adam G, Gibbs JH (1965) J Chem Phys 43(1):139
20. Boyer RF (1963) Rubber Chem Technol 46:1303
21. Hale A, Macosko CW, Bair HE (1991) Macromolecules 24:2610
22. Lovell R, Windle AH (1990) Polymer 31(4):593
23. Wu Wl, Bauer BJ (1986) Polymer 27:169
24. Arruda EM, Boyce MC (1993) Int J Plasticity 9:697
25. Kovacs AJ, Aklonis JJ, Hutchinson JM, Ramos AR (1979) J Polym Sci: B Polym Phys 17:1097
26. Lesser AJ, Calzia KJ (2004) J Polym Sci B: Polym Phys 42:2050
27. Crawford ED, Lesser AJ (1998) J Polym Sci: B Polym Phys 36:1371
28. van Melick HGH, Govaert LE, Meijer HEH (2003) Polymer 44:2493
29. Cross A, Haward RN (1978) Polymer 19:677
30. Treloar LRG (1975) The physics of rubber elasticity. Clarendon Press, Oxford
31. Arruda EM, Boyce MC, Jayachandran R (1995) Mech Mater 19:193
32. Haward RN, Thackray G (1968) Proc R Soc Lond A 302:453
33. Tervoort TA, Govaert LE (2000) J Rheol 44(6):1263
34. Charlesworth JM (1988) Polym Eng Sci 28(4):230
35. Porter RS, Johnson JF (1966) Chem Rev 66(1):1
36. Hoy RS, Robbins MO (2006) J Polym Sci: B Polym Phys 44:3487
37. Haward RN, Young RJ (1997) The physics of glassy polymers. Chapman and Hall, New York
38. Wendlandt M, Tervoort TA, Suter UW (2010) J Polym Sci: B Polym Phys 48:1464

39. Govaert LE, Engels TAP, Wendlandt M, Tervoort T, Suter UW (2008) J Polym Sci: B Polym Phys 46:2475
40. Lesser AJ, Crawford E (1997) J Appl Polym Sci 66:387
41. Fox TG, Loshaek S (1955) J Polym Sci 15:371
42. Espuche E, Galy J, Gerard JF, Pascualt JP, Sautereau H (1995) Macromol Symp 93:107
43. Robertson RE (1966) J Chem Phys 44(10):3950
44. Calzia KJ, Lesser AJ (2007) J Mater Sci 32:5229. doi:10.1007/s10853-006-1268-0
45. Bree HW, Heijboer J, Struik LCE, Tak AGM (1974) J Polym Sci: B Polym Phys 12:1857
46. Charlesworth JM (1988) Polym Eng Sci 28(4):221
47. G'Sell C, McKenna GB (1992) Polymer 33(10):2103
48. Wang X, Gillham JK (1993) J Appl Polym Sci 47:447
49. Boyce MC, Arruda EM (2000) Rubber Chem Technol 73(3):504
50. Rivlin RS, Saunders DW (1951) Philos Trans R Soc Lond A 243:251
51. Bicerano J (2002) Prediction of polymer properties, 3rd edn. Marcel Dekker, Inc., New York
52. Bicerano J, Sammler RL, Carriere CJ, Seitz JT (1996) J Polym Sci: B Polym Phys 34:2247